Nanoparticle-based endodontic antimicrobial photodynamic therapy

Tom C. Pagonis, DDS, MS, **Judy Chen, DDS**, **Carla Raquel Fontana, DDS, PhD**, **Harikrishna Devalapally, PhD**, **Karriann Ruggiero, BS**, **Xiaoqing Song, MD, MS**, **Federico Foschi, DDS, PhD**, **Joshua Dunham, BS**, **Ziedonis Skobe, PhD**, **Hajime Yamazaki, MS**, **Ralph Kent, ScD**, **Anne C.R. Tanner, BDS, PhD**, **Mansoor M. Amiji, PhD**, and **Nikolaos S. Soukos, DDS, PhD**
Dr. Pagonis is Clinical Instructor and Dr. Chen is a resident in Advanced Graduate Endodontics, Division of Endodontics, Harvard School of Dental Medicine, Boston, Massachusetts; Drs. Fontana and Foschi are postdoctoral research fellows, Ms. Ruggiero and Mr. Dunham are research assistants, and Dr. Song is a research fellow, Applied Molecular Photomedicine Laboratory, The Forsyth Institute, Boston, Massachusetts; Dr. Skobe is Head of the Biostructure Core Facility/ Department of Biomineralization, Mr. Hajime Yamazaki is a Research Assistant, Department of Biomineralization, Dr. Tanner is Senior Scientist, Department of Molecular Genetics and Dr. Kent is Head of the Department of Biostatistics, The Forsyth Institute; Dr. Devalapally is a postdoctoral research fellow and Dr. Amiji is Head of Department of Pharmaceutical Sciences, School of Pharmacy, Bouvé College of Health Sciences, Northeastern University, Boston, Massachusetts; Dr. Soukos is the Director of the Applied Molecular Photomedicine Laboratory, The Forsyth Institute

Abstract

Objective—To study the *in vitro* effects of poly(lactic-co-glycolic acid) (PLGA) nanoparticles loaded with the photosensitizer methylene blue (MB) and light against *Enterococcus faecalis* (ATCC 29212).

Materials and Methods—The uptake and distribution of nanoparticles in *E. faecalis* in suspension was investigated by transmission electron microscopy (TEM) after incubation with PLGA complexed with colloidal gold particles for 2.5, 5 and 10 minutes. *E. faecalis* species were sensitized in planktonic phase and in experimentally infected root canals of human extracted teeth with MB-loaded nanoparticles for 10 minutes followed by exposure to red light at 665 nm.

Results—The nanoparticles were found to be concentrated mainly on the cell walls of microorganisms at all three time points. The synergism of light and MB-loaded nanoparticles led to approximately 2 and 1 $\log_{10}$ reduction of colony-forming units in planktonic phase and root canals, respectively. In both cases, mean $\log_{10}$ CFU levels were significantly lower than controls and MB-loaded nanoparticles without light.

Conclusion—The utilization of PLGA nanoparticles encapsulated with photoactive drugs may be a promising adjunct in antimicrobial endodontic treatment.

Keywords

photodynamic therapy; methylene blue; polymeric nanoparticles; endodontic disinfection; *Enterococcus faecalis*

INTRODUCTION

The goal of endodontic treatment is to prevent and, when required, to eliminate endodontic infection and allow healing of apical periodontitis (1). Although the bulk of the infecting microorganisms are removed during chemomechanical debridement, residual bacteria are readily detectable in approximately one-half of teeth at the time of obturation (2). The complexity of the root canal system with its isthmuses, ramifications, and dentinal tubules make complete debridement of bacteria almost impossible, even when conventional methods of endodontic instrumentation and irrigation are performed to the highest technical standards (3). Furthermore, scanning electron microscopic investigations have demonstrated bacterial penetration up to 1000 μm into dentinal tubules (4). The presence of a 'smear layer' during and after instrumentation reduces the effectiveness of irrigants and intracanal medicaments in disinfecting dentinal tubules (5). Nonsurgical endodontic treatment failures are associated with high proportions of gram-positive aerobic and facultative organisms, versus the predominance of strict anaerobes in primary endodontic infections (6,7). *Enterococcus faecalis* microorganisms, which are rarely found in large proportions in primary endodontic infections, are highly associated with endodontic failures (8,9), and show resistance to common intracanal medications (10). Disinfection of the root canal system is critical to success and the need for better root canal disinfection is clear and compelling.

The use of photodynamic therapy (PDT) for inactivation of microorganisms was first demonstrated more than 100 years ago, when Oscar Raab reported the lethal effect of acridine hydrochloride on *Paramecia caudatum* (11). PDT is based on the concept that non-toxic photosensitizers can be preferentially localized in certain tissues and subsequently activated by light of the appropriate wavelength to generate singlet oxygen and free radicals that are cytotoxic to cells of the target tissue (12). Methylene blue (MB) is a well-established photosensitizer that has been used in PDT for targeting various gram-positive and gram-negative oral bacteria (13) and was previously employed to study the effect of PDT on endodontic disinfection (14-20). Several studies have demonstrated incomplete destruction of oral biofilms using MB-mediated PDT (21-24). The reduced susceptibility of biofilms to PDT was attributed to reduced penetration of the dye (21,22). In addition, it has been shown that phenothiazinium-based photosensitizers, including MB and toluidine blue O, are substrates of multi-drug resistance pumps in bacteria thus decreasing the effectiveness of the photosensitizer (25). Therefore, one of the ways to overcome these deficiencies is to develop drug delivery systems that significantly improve the pharmacological characteristics of MB.

Recently, studies in PDT have focused on the use of polymer-based nanoparticles for photosensitizer delivery and release systems. Nanoparticles containing photosensitizers have several advantages over photosensitizing molecules not encapsulated in nanoparticles. These advantages include (26): 1) A larger critical mass (concentrated package of photosensitizer) for the production of reactive oxygen species that destroy cells, 2) Limit the target cell's ability to pump the drug molecule back out thus reducing the possibility of multiple-drug-resistance, 3) Selectivity of treatment by localized delivery agents, which can be achieved by either passive targeting or by active targeting via the charged surface of the nanoparticle, and 4) The nanoparticle matrix is non-immunogenic. Engineered biodegradable polymeric nanoparticles, made of FDA-approved poly(lactic-*co*-glycolic acid) (PLGA) (27), were used as a drug delivery system for photosensitizers (28-30). Once encapsulated within PLGA, the excited

state of the photosensitizer is quenched, which results in loss of phototoxicity (29). When the nanoparticles were incubated with the targeted cells, they showed a time-dependent release of the photosensitizer, which then regained its phototoxicity and resulted in an activatable PDT-nanoagent (29). Although PLGA nanoparticles loaded with various compounds (e.g. antibiotics) have been used for bacterial targeting (31,32), the use of PLGA nanoparticles as carriers of photosensitizers has not been previously explored in antimicrobial PDT.

The objective of the present study was to use MB-loaded PLGA nanoparticles for *in vitro* evaluations against *E. faecalis*. We also explored the photodynamic effects of these nanoparticles in targeting *E. faecalis* biofilms in experimentally infected root canals of extracted teeth. Our hypothesis was that the encapsulation of MB within PLGA nanoparticles (~150–200 nm in diameter) may offer a novel design of nanoplatform for enhanced drug delivery in the root canal system and photodestruction of root canal biofilms.

MATERIALS AND METHODS

Preparation of PLGA nanocarriers

Medical grade PLGA (MW 12 KDa, 50:50 lactide-glycolide molar ratio) was obtained from Birmingham Polymers (Pelham, AL). Pluronic® F-108, an ABA triblock copolymer of poly (ethylene oxide) (PEO) and poly(propylene oxide) (PPO) was kindly supplied by the Performance Chemicals Division of BASF Corporation (Parsipanny, NJ). Both blank and MB-loaded (10% w/w) PLGA nanoparticles were prepared by blending the polyester with Pluronic® F-108 triblock copolymer and fabricating the nanoparticles by a solvent displacement procedure as previously reported (33). Briefly, a solution of PLGA (76 mg) and Pluronic® F-108 (14 mg) was prepared in acetone (5 ml) and heated with stirring until it became clear. This was introduced into an aqueous (50 ml) solution under vigorous magnetic stirring. The rate of addition of organic phase (1ml/min) to aqueous phase, volume ratios, and the stirring speed was optimized to ensure batch-to-batch reproducibility. After overnight stirring, the nanoparticle was centrifuged at 10000 rpm for 20 min, and then washed twice with water and freeze dried. For the preparation of the nanocarrier formulations, MB and sodium oleate were purchased from Sigma Chemicals (St. Louis, MO). The oleate salt of MB was dissolved at 10% (w/w) concentration in the acetone solution of PLGA. Pluronic® triblock copolymers were added to the polymer solution in acetone at 20% (w/w). The concentration and type of Pluronic® triblock copolymer was optimized to insure that the formed nanocarriers have a stable hydrophilic surface, which resists aggregation.

Characterization of PLGA nanocarriers

The mean size of PLGA nanoparticles, with and without the encapsulated payloads, was determined via laser light scattering using a ZetaPALS system (Brookhaven Instruments, Holtsville, NY). After freeze-drying, the surface morphology of the nanocarriers was visualized using field emission scanning electron microscopy (Shimadzu, Japan). The surface charge on the nanocarriers, in the absence and presence of encapsulated payload, was determined by zeta potential measurements. Zeta potential measurements of the nanocarrier suspensions in phosphate-buffered saline (PBS, pH 7.4) were done with Brookhaven Instruments (Holtsville, NY) and ZetaPALS (Phase Analysis Light Scattering) ultra-sensitive zeta potential analyzer. To determine the amount of drug loaded into the nanocarriers (capacity) as well as the percentage of added drug (efficiency), a known amount (~10 mg) of the control and PEO-modified nanocarriers was dissolved in acetone. The amount of encapsulated drug in the nanocarriers was determined by using the UV-VIS absorbance of MB. The release kinetics of MB-oleate from the nanoparticles was determined in PBS (pH 7.4). Tween®-80, a non-ionic surfactant, at 1.0% (w/v) concentration, was added to the release medium to enhance the solubility of MB-oleate complex and to prevent the drugs from binding to the container

surface. One-hundred mg of the drug-containing nanocarriers was incubated with 10 mL of the release medium in a shaking water-bath (50 rpm). Periodically, 5 ml of the release medium was removed and replaced with 5 mL of fresh buffer to maintain sink conditions. Methylene blue in the release medium was assayed by a Shimadzu UV-VIS spectrophotometer (Columbia, MD). Cumulative amount and percent drug released was determined from appropriate calibration curves of the respective agents.

Bacterial culture

Enterococcus faecalis (ATCC 29212) was used in this study. Cultures were maintained by weekly subculture in plates comprised of trypticase soy agar (Becton, Dickinson, and Co., Sparks, MD) with 5% sheep blood (Northeast Laboratories, Waterville, ME). For experimental purposes, the microorganism was grown in the presence of 80% N_2, 10% H_2, 10% CO_2 at 35° c in an anaerobic chamber for 72 hr; harvested from plates; and re-suspended in brain heart infusion (BHI) broth. Cells were dispersed by vortexing and repeated passage through Pasteur pipettes. Cell numbers were measured in a spectrophotometer (wavelength, 600 nm; 0.1 optical density unit equals approximately 10^8 cells/ml) in 1-ml cuvettes.

Bacterial uptake of nanoparticles

The uptake and distribution in *E. faecalis* was investigated by transmission electron microscopy (TEM) using PLGA complexed with colloidal gold particles. Colloidal gold nanoparticles (10–15 nm) were prepared by reduction of chloroauric acid with sodium citrate. To a flask containing 85 mL of boiling HPLC water, Cloroauric acid (HAuCl4) solution (10 mL, 5mM) was added, and the solution was allowed to return to a boil. A freshly prepared solution of sodium citrate (5 mL, 0.03 M) was then added to the flask. After a few minutes, the solution turned from colorless to a deep wine-red color. Heating was stopped at this point and the resulting sol was left to cool overnight. The nanoparticles were centrifuged at 30000 rpm for 10 min and the supernatant was discarded. The remaining pellet was re-dispersed in deionized distilled water for further use. The physical properties of the nanoparticles, such as size and zeta potential, were compared with those of unloaded nanoparticles and were not found to be significantly different. Bacteria (10^8/ml) were incubated with PLGA-Au-Pluronic® nanoparticle suspension (100 μg/ml) for 2.5, 5 and 10 min, centrifuged and washed twice with phosphate buffered saline (PBS). Then, microorganisms were fixed in 2.5% glutaraldehyde solution at room temperature for 1 hour, washed with distilled water, and postfixed in 1% osmium tetroxide and uranyl acetate. The cells were dehydrated with ethanol and embedded in Epon®. Thin-sectioned samples were prepared and examined using a transmission electron microscope (Brand Inc., City, ST).

Photodynamic treatment of bacterial suspensions

For the photodynamic treatment of microorganisms, aliquots of bacterial suspensions (10^8/ml) were placed in sterile microcentrifuge tubes and were centrifuged (7000rpm for 4 minutes). The supernatants were aspirated and 1 ml of BHI with MB-loaded PLGA nanoparticles (final concentration: 6.25 μg/ml equivalent to MB) was then added. Cultures were resuspended with the nanoparticles and placed in the wells of 24-well plates for 10 min before they were exposed to light. All wells were irradiated with red light from a diode laser (BWTEK Inc., Newark, DE) with an output power of 1 Watt and a central wavelength of 665 nm for 10 min in the dark at room temperature. The system was coupled to an optical fiber 1 mm in diameter that delivered light into a lens. This formed a uniform circular spot on the base of the 24-well plate, 2cm in diameter. The laser possessed a spectral stability of $\pm$ 2 nm with an output power stability of 10 mW. Power measurements were quantified with a power meter (Ophir Optronics LTD, Danvers, MA). Distance adjustments between the lens and the illuminated plates created fields of irradiation with appropriate dimensions and power densities. The light exposure was from

above with an irradiance of 100 mW/cm^2 and an energy fluence of 60 J/cm.^{2} All plates were kept covered during the illumination in order to maintain the purity of the culture. After illumination of the appropriate wells, bacterial suspensions underwent serial dilutions in BHI broth and 100 μl aliquots were plated on blood agar plates for anaerobic incubation for 7 days. The following experimental groups were used: 1) No light/No MB-nanoparticles (control), 2) Treated only with MB-loaded nanoparticles, and 3) Treated with MB-loaded nanoparticles and light. Three separate experiments were carried out with 4 bacterial cultures per group in each experiment. The primary endpoint for evaluation was the mean number of colony-forming units (CFU) per group.

Preparation of tooth specimens

Thirty-two freshly extracted single-rooted human teeth were stored in 0.5% sodium hypochlorite (NaOCl) for 2 weeks. Specimens were decoronated to a standard 12 mm root segment length with a rotating diamond saw (#911H, Brasseler USA, Savannah, GA) set at 20,000 rpm under water-coolent. Patency of apical foramina was established by inserting a size 15K-file (Dentsply Maillefer, Tulsa, OK). A file measurement was taken at the point where the size 15 K-file became visible at the apical foramen and 0.5 mm was subtracted to set the working length. The instrumentation sequence consisted of: Gates Glidden Burs (Dentsply Maillefer, Tulsa, OK) sizes 4 and 2 for the coronal 4 mm, ProTaper® S1 (Dentsply Tulsa Dental, Tulsa, OK), followed by .06 taper Profile® series 29® (Dentsply Tulsa Dental, Tulsa,OK) files sizes 4 (0.216 ISO equivalent) to 7 (0.465 ISO equivalent) in a crown-down manner, to achieve a master apical file size of 0.465 (ISO equivalent). An Aseptico Endo ITR™ (Dentsply Tulsa Dental, Tulsa, OK) electric motor was used with an 8:1 gear reduction mini-head contra-angle. Final apical patency was established with a size 25 K-file (Dentsply Maillefer, Tulsa, OK) in order to allow for an adequate apical aperture for flushing of microbial aggregates. RC Prep® (Premium Products, Plymouth Meeting, PA) was used as a lubricant and canals were irrigated with 6% sodium hypochlorite (NaOCl) throughout the instrumentation sequence. Final irrigation consisted of 1 ml of 17% ethylene diamine tetraacetic acid (EDTA) solution for 3 min for smear layer removal, deactivated with 1 ml of 6% NaOCl for 3 minutes. Each tooth specimen was then placed in a microcentrifuge tube containing 500 μl of phosphate buffered saline (PBS). Teeth were subsequently autoclaved at 121°C for 20 minutes. Following autoclave sterilization, PBS was aspirated from the microcentrifuge tubes under sterile conditions. The root surface was coated with Performix (Plasti Dip, Blaine, MN) to avoid external microbial contamination.

Infection of root canals

Twenty-six root specimens were transferred into sterile microcentrifuge tubes under sterile conditions. One milliliter of BHI broth containing 10^9 microorganisms of *E. faecalis* was injected into the prepared root canal system using a ProRinse® 30 gauge irrigation needle (Dentsply Tulsa Dental, Tulsa, OK). After injection, each specimen was entirely submerged in BHI broth, and the tubes were incubated anaerobically for 3 days. Following incubation, the medium was aseptically aspirated from the tubes. Three specimens were processed for SEM studies and 23 specimens were used for PDT studies.

Scanning Electron Microscopy (SEM)

A total of 9 human extracted teeth with a single canal were randomly selected for SEM. Three specimens were used for demonstration of the smear layer removal and the patency of dentinal tubules and three specimens for demonstration of *E. faecalis* infection. The root canals of three uninfected specimens were incubated with 1 ml PBS containing MB-loaded nanoparticles (final concentration: 50 μg/ml equivalent to MB) for 15 min to demonstrate the delivery of nanoparticles in the root canal system. Longitudinal grooves were cut with a diamond bur both

on palatal/lingual and buccal surfaces of each root to facilitate vertical splitting with a chisel. Each sample was split into two halves with a stainless steel chisel. The sample half with the most visible part of the apex was fixed in 3.7% glutaraldehyde in 0.2 M sodium cacodylate buffered solution at 4°C for 24 hours. After dehydration in a graded ethanol concentration series, samples were air dried and mounted on an SEM stubs for gold sputtering and observation with a JEOL JSM 6400 scanning electron microscope (JEOL Corporation, Tokyo, Japan). SEM microphotographs were obtained at a standard magnification of 1500x at each third (coronal, middle and apical) and on the fracture surface.

Photodynamic treatment of root canal biofilms

Twenty-three root specimens were prepared and infected as described above, and were subjected to PDT using MB-loaded nanoparticles in BHI broth. The specimens were randomly assigned to the following three groups: 1) No light/No MB-nanoparticles, 2) Treated only with MB-loaded nanoparticles, and 3) Treated with MB-loaded nanoparticles and light. Two separate experiments were carried out with 4 specimens per group in each experiment with the exception of the group treated only with MB-loaded nanoparticles, in which 4 and 3 specimens were used, respectively. All individual specimens were placed in 1.5 ml microcentrifuge tubes under sterile conditions and then the canals of the MB-loaded nanoparticles only and PDT groups were filled to the level of the access cavity with nanoparticle solution (final concentration: 50 μg/ml equivalent to MB) using a Pro Rinse® 30 gauge irrigation needle (Dentsply Tulsa Dental). After injection, the entire specimen was fully immersed in the solution for 15 minutes so that the root canal system will be continuously exposed to the drug. In a clinical setting, the drug will be applied in the root canal and taken up by residual bacteria in the main root canal, isthmuses, lateral canals and dentinal tubules. To minimize the *in vitro* impact of the drug escaping from the apex we attempted to mimic the continuous in vivo clinical presence of the drug during non-surgical endodontic treatment by fully immersing the root specimen in the drug solution in order to provide the continuous intracanal presence of MB. In addition, the Performix coating eliminated any possible seepage of MB from the root surface. Specimens in the control groups were injected and fully immersed in sterile BHI broth. Following incubation, excess drug solution was aspirated and the root specimens were removed from the tubes. Light was then applied in the root canal system of the specimens for 5 min. The irradiation source was a diode laser (BWTEK Inc., Newark, DE) with an output power of 1 Watt and a central wavelength of 665 nm. The system was coupled to a 250-μm diameter poly(methylmethacrylate) optical fiber that was mechanically notched over a one-centimeter length at approximately one-millimeter intervals (Schoelly Imaging Inc., Worcester, MA). The fiber was able to uniformly distribute light at 360° (Fimple et al., 2008). The power density was 100 mW/cm^2 and the total energy fluence dose was 30 J/cm^2. Following all treatments, each specimen was aseptically mounted on a rubber dam, by utilizing a plastic u-shaped rubber dam frame (Hygienic brand, Coltene/Whaledent, Cuyahoga Falls, Ohio) attached to a rack and oriented parallel to the lab bench top. The coronal 4 mm of each specimen was above the surface of the dam. The contents of root canals were sampled by flushing the root canals with a coronal application of 1-ml of BHI broth with a Pro Rinse® 30 gauge irrigation needle (Dentsply Tulsa Dental). The bacterial suspension was collected in a 1.5 ml microcentrifuge tube positioned below the apical foramen and bacterial yielding was measured spectrophotometrically for each sample (the reading for BHI alone was subtracted). After vortexing for 20 seconds, serial dilutions were prepared and 100 μl aliquots were inoculated onto blood agar and incubated anaerobically for 7 days.

Data analysis

In three PDT experiments of bacterial suspensions, two treatments (MB-loaded nanoparticles alone and Light plus MB-loaded nanoparticles) and a Control were evaluated. Four observations (CFU counts) were obtained for each treatment group in each of the three

experiments, a total of 12 observations per treatment and 36 observations overall. Data values were $\log_{10}$ transformed to reduce variance heterogeneity. Treatment effects on $\log_{10}$ CFU levels were evaluated in a two-way analysis of variance (3 experiments X 3 treatments) in order to control any extraneous variation from experiment to experiment, while obtaining summary comparisons of treatment effects. Pairwise comparisons of mean treatment levels were done by Tukey's multiple comparisons procedure with overall alpha=0.01. In the case of the root canal data, a similar analysis was performed for $\log_{10}$ CFU values, in this case with two experiments and again with 4 observations for each treatment group, a total of 8 observations per treatment and 24 observations overall (2 experiments X 3 treatments). Following the ANOVA, pairwise comparisons of treatment effects were again done by Tukey's procedure with overall alpha=0.01. Treatment means and standard errors in Figure 3 are based on pooling all values for each treatment from three experiments and in Figure 5 pooling all values from two experiments.

RESULTS

Characterization of nanoparticles

The diameter of PEO-PLGA nanoparticles ranged from 100 to 250 nm. The particle size remained the same with inclusion of MB. The surface charge of the nanocarriers, in the absence and presence of encapsulated payload, was determined by zeta potential measurements and was found to be −23.48 and −31.87 mV, respectively. These average values were obtained from 6 independent batches of nanoparticles and were not statistically significant (p>0.05). After freeze-drying, the surface morphology of the nanocarriers was visualized by SEM. PLGA nanoparticles were spherical in shape and had a smooth surface (Fig. 1). UV-visible spectroscopy verified the capacity and efficiency of MB encapsulation.

Transmission electron microscopy studies

The uptake and distribution of nanoparticles in *E. faecalis* was investigated by TEM using PLGA complexed with colloidal gold particles (10–15 nm) in order to obtain high contrast. Following incubation of microorganisms with a suspension (100 μg/ml) of PLGA-Au-Pluronic® nanoparticles for up to 10 min, TEM revealed substantial accumulation of nanoparticles on bacterial cell walls (**Fig. 2**, b-d). The surface properties (size and charge) of nanoparticles were the same for either gold or MB.

Photosensitization of *E. faecalis* in planktonic phase

Mean $\log_{10}$ CFU levels, summarized for all three experiments in Fig. 3, were highest for Control, slightly lower for MB-loaded nanoparticles alone and markedly lower for the combination of Light with MB-loaded nanoparticles. This same pattern of progressively lower mean levels was observed in all three experiments. Treatment main effects in the two-way Anova were highly significant (P<0.0001). Pairwise comparisons among treatment means by Tukey's multiple comparisons procedure with overall alpha=0.01 indicated that MB-loaded nanoparticles were not significantly lower than Control and that Light with MB-loaded nanoparticles was significantly lower than both Control and MB-loaded nanoparticles alone. Survival fractions relative to Control levels (Mean CFU= 259.5), computed separately for each experiment and then averaged over the three experiments, were 66.1% for MB-loaded nanoparticles and 3.3% for Light with MB-loaded nanoparticles. In separate experiments, bacterial viability was not reduced when microorganisms were treated with either only light or only with unloaded nanoparticles (data not shown).

Scanning electron microscopy studies

SEM demonstrated open dentinal tubules after the removal of the smear layer with NaOCl and EDTA (**Fig. 4**, A). Three days after inoculation with *E. faecalis*, a dense infection occurred in the root canal (**Fig. 4**, B). SEM also demonstrated the delivery of spherically shaped MB-loaded PLGA nanoparticles in the root canal system (**Fig 4**, C).

Photosensitization of root canal biofilm bacteria

Results for root canal experiments (Fig. 5) followed a similar pattern to that seen in the planktonic experiments. Treatment main effects in the two-way Anova were highly significant (P<0.0001). Pairwise comparisons among treatment means with overall alpha=0.01 indicated that both MB-loaded nanoparticles only and Light with MB-loaded nanoparticles were both significantly lower than Control. In addition, Light with MB-loaded nanoparticles was significantly lower than MB-loaded nanoparticles. Survival fractions relative to mean CFU for Control levels (Mean CFU= 260.4) were 41.5% for MB-loaded nanoparticles and 15.2% for Light with MB-loaded nanoparticles.

DISCUSSION

Polymer-based nanoparticles have recently been used for delivery of photosensitizers and release systems, in particular those with biocompatible and biodegradable polymers. These systems are able to target different organs and control the release of the photosensitizer molecules by the incorporation of site-specific moieties, e.g. the modification of the particles' surface with poly(ethylene oxide) to improve the carrier's biocompatibility and biodistribution (33-35). The present study explored a new approach for antimicrobial therapy against the microorganism *E. faecalis* with light activation of targeted MB-loaded PLGA nanoparticles. Our goals were to investigate: a) the susceptibility of *E. faecalis* species in planktonic phase; and b) the ability of nanoparticles to deliver MB in the root canal system and root canal biofilms of experimentally infected teeth enabling their elimination by PDT. The nanoparticle matrix PLGA is a polyester co-polymer of polylactic acid (PLA) and polyglycolic acid (PGA) that has received FDA approval due to its biocompatibility and its ability to degrade in the body through natural pathways (36). Methylene blue has previously been encapsulated into polyacrylamide, sol-gelica silica and organically modified silicate nanoparticles for phototargeting tumor cells *in vitro* (37). Recently, MB-containing silica-coated magnetic nanoparticles were proposed as potential carriers for PDT (38).

The susceptibility of *E. faecalis* species to PDT mediated by MB-loaded PLGA nanoparticles was investigated in planktonic phase. Sensitization of *E. faecalis* species with nanoparticles (6.25 µg/mL equivalent to MB) followed by exposure to red light at 665 nm with energy fluence of 60 J/cm^2 led to approximately 2 $\log_{10}$ bacterial killing. In addition, the synergism of nanoparticles (50 µg/mL equivalent to MB) and light (30 J/cm^2) exhibited approximately 1 $\log_{10}$ killing of *E. faecalis* biofilm species in experimentally infected root canals of human extracted teeth. In both planktonic and root canal experiments, MB-loaded nanoparticles alone exhibited approximately 44% and 58% reduction of bacterial viability, respectively. In the present study, the effect of light alone in root canals was not investigated. A previous study conducted by our group did not show a significant effect of light on bacterial viability compared with controls (no light/no drug) (18). Although direct comparisons between results obtained from planktonic and root canal experiments cannot be made, both experimental conditions clearly demonstrate the bacterial susceptibility to PDT induced by MB-loaded PLGA nanoparticles. A complete evaluation of the photodynamic effects of MB-loaded nanoparticles on root canal biofilms would also require knowledge of optimum treatment parameters. These include the concentration of MB encapsulated in nanoparticles, the incubation time of nanoparticles with microorganisms, the power density and energy fluence of light. TEM

demonstrated that nanoparticles were mainly concentrated on bacterial cell walls. This may have rendered the cell wall permeable to MB (39) released by the nanoparticles. In this case, the intracellular localization and the local surroundings of MB influence the phototoxicity. Sensitization of MB with light leads to the production of singlet oxygen ($^1O_2$), which can migrate approximately 0.02 μm after its formation, targeting important intracellular components (12). There is also another scenario, according to which photodestruction takes place within the cell wall. In this case the intracellular content may have leaked out. However, the fact that MB-loaded nanoparticles alone exhibited a toxicity ranging from 34% to 58.5% suggests that MB penetrated the bacterial cell well.

The photodynamic effects of MB-loaded PLGA nanoparticles on *E. faecalis* were probably affected by the presence of serum proteins in brain-heart infusion broth (40-42). Preliminary results obtained in our laboratory from PDT studies using MB-loaded PLGA nanoparticles for targeting *E. faecalis in vitro* demonstrate greater bacterial killing when these nanoparticles are dissolved in phosphate buffered saline (unpublished data). Recently, it was found that MB dissolved in a mixture of glycerol:ethanol:water (17) as well as a MB formulation containing an emulsion of oxidizer:oxygen carrier (19) enhanced the photodynamic effects of MB *in vitro*. A limitation of the present study is related to the sampling method used for the collection of biofilm species from root canals. Flushing with medium leads to detachment of biofilm species mainly from the surface of the root canal and the openings of dentinal tubules. In preliminary studies, we used paper points, but fewer bacteria were obtained compared with flushing. We also crushed the root specimens (cryopulverization) in order to assay the fragments. The data obtained were not convincing. The flushing method was preferred over files in order to avoid bacterial destruction induced by the latter.

The use of a biodegradable polymer to synthesize the nanoparticles makes the final product attractive for clinical use. Future studies should define the treatment parameters for optimum endodontic disinfection and the therapeutic window where microorganisms could be killed by MB-loaded nanoparticles while sparing normal cells. The role of nanoparticle surface charge on antimicrobial PDT effect should also be evaluated. At a later stage, a comparison between the photodynamic effects of MB-loaded nanoparticles and free MB would be necessary.

Acknowledgments

REFERENCES

1. Ørstavik, D.; Pitt Ford, TR. Apical periodontitis. Microbial infection and host responses. In: Ørstavik, D.; Pitt Ford, TR., editors. Essential Endodontology: Prevention and Treatment of apical periodontitis. Blackwell Science; 1998.

2. Byström A, Sundqvist G. Bacteriologic evaluation of the effect of 0.5 percent sodium hypochlorite in endodontic therapy. Oral Surg Oral Med Oral Pathol 1983;55:307–12. [PubMed: 6572884]

3. Siqueira JF Jr, Araújo MCP, Garcia PF, Fraga RC, Dantas CJS. Histological evaluation of the effectiveness of five instrumentation techniques for cleaning the apical third of root canals. J Endod 1997;23:499–502. [PubMed: 9587319]

4. Haapasalo M, Ørstavik D. *In vitro* infection and disinfection of dentinal tubules. J Dent Res 1987;66:1375–9. [PubMed: 3114347]

5. Berutti E, Marine R, Angeretti A. Penetration ability of different irrigants into dentinal tubules. J Endod 1997;23:725–7. [PubMed: 9487845]

6. Rolph HJ, Lennon A, Riggio MP, Saunders WP, MacKenzie D, Coldero L, Bagg J. Molecular identification of microorganisms from endodontic infections. J Clin Microbiol 2001;39:3282–9. [PubMed: 11526164]

7. Siqueira JF, Rocas IN. Nested PCR detection of *Centipeda periodontii* in primary endodontic infections. J Endod 2004;30:135–7. [PubMed: 15055428]

8. Foschi F, Cavrini F, Montebugnoli L, Stashenko P, Sambri V, Prati C. Detection of bacteria in endodontic samples by polymerase chain reaction assays and association with defined clinical signs in Italian patients. Oral Microbiol Immunol 2005;20:289–95. [PubMed: 16101964]

9. Radcliffe CE, Potouridou L, Qureshi R, Habahbeh N, Qualtrough A, Worthington H, Drucker DB. Antimicrobial activity of varying concentrations of sodium hypochlorite on the endodontic microorganisms Actinomyces israelii, A. naeslundii, Candida albicans and *Enterococcus faecalis*. Int Endod J 2004;37:438–46. [PubMed: 15189432]

10. Distel JW, Hatton JF, Gillespie MJ. Biofilm formation in medicated root canals. J Endod 2002;28:689–93. [PubMed: 12398165]

11. Raab O. Über die Wirkung Fluoreszierender Stoffe auf Infusorien. Z Biol 1900;39:524–46.

12. Dougherty TJ, Gomer CJ, Henderson BW, Jori G, Kessel D, Korbelik M, Moan J, Peng Q. Photodynamic therapy. J Natl Cancer Inst 1998;90:889–905. [PubMed: 9637138]

13. Harris F, Chatfield LK, Phoenix DA. Phenothiazinium based photosensitisers-photodynamic agents with a multiplicity of cellular targets and clinical applications. Curr Drug Targets 2005;6:615–27. [PubMed: 16026282]

14. Soukos NS, Chen PS, Morris JT, Ruggiero K, Abernethy AD, Som S, Foschi F, Doucette S, Luschke Bammann L, Raquel Fontana C, Doukas AG, Stashenko PP. Photodynamic therapy for endodontic disinfection. J Endod 2006;32:979–84. [PubMed: 16982278]

15. Foschi F, Fontana CR, Ruggiero K, Riahi R, Vera A, Doukas AG, Pagonis TC, Kent R, Stashenko PP, Soukos NS. Photodynamic inactivation of *Enterococcus faecalis* in dental root canals *in vitro*. Lasers Surg Med 2007;39:782–87. [PubMed: 18081066]

16. George S, Kishen A. Advanced noninvasive light-activated disinfection: assessment of cytotoxicity on fibroblast versus antimicrobial activity against *Enterococcus faecalis*. J Endod 2007;33:599–602. [PubMed: 17437881]

17. George S, Kishen A. Photophysical, photochemical, and photobiological characterization of methylene blue formulations for light-activated root canal disinfection. J Biomed Opt 2007;12:034029. [PubMed: 17614737]

18. Fimple JL, Fontana CR, Foschi F, Ruggiero K, Song X, Pagonis TC, Tanner R, Kent ACR, Doukas AG, Stashenko PP, Soukos NS. Photodynamic treatment of endodontic polymicrobial infection *in vitro*. J Endod 2008;34:728–34. [PubMed: 18498901]

19. George S, Kishen A. Augmenting the antibiofilm efficacy of advanced noninvasive light activated disinfection with emulsified oxidizer and oxygen carrier. J Endod 2008;34:1119–23. [PubMed: 18718378]

20. Lim Z, Cheng JL, Lim TW, Teo EG, Wong J, George S, et al. Light activated disinfection: an alternative endodontic disinfection strategy. Aust Dent J 2009;54:108–14. [PubMed: 19473151]

21. Soukos NS, Socransky SS, Mulholland SE, Lee S, Doukas AG. Photomechanical drug delivery into bacterial biofilms. Pharm Res 2000;17:405–409. [PubMed: 10870983]

22. Ogura MAA, Blissett R, Ruggiero K, Som S, Goodson J, Kent R, Doukas A, Soukos N. Photomechanical wave-assisted molecular delivery in oral biofilms. World J Microbiol Biotechnol 2007;23:1637–46.

23. Müller P, Guggenheim B, Schmidlin PR. Efficacy of gasiform ozone and photodynamic therapy on a multispecies oral biofilm *in vitro*. Eur J Oral Sci 2007;115:77–80. [PubMed: 17305720]

24. Fontana CR, Abernethy AD, Som S, Ruggiero K, Doucette S, Marcantonio RC, Boussios CI, Kent R, Goodson JM, Tanner ACR, Soukos NS. The antibacterial effect of photodynamic therapy in dental plaque-derived biofilms. J Periodontal Res. In Press.

25. Tegos GP, Hamblin MR. Phenothiazinium antimicrobial photosensitizers are substrates of bacterial multidrug resistance pumps. Antimicrob Agents Chemother 2006;50:196–203. [PubMed: 16377686]

26. Koo YEL, Fan W, Hah H, Xu H, Orringer D, Ross B, Rehemtulla A, Philbert MA, Kopelman R. Photonic explorers based on multifunctional nanoplatforms for biosensing and photodynamic therapy. Appl Optics 2007;46:1924–30.

27. Langer R. Drug delivery and targeting. Nature 1998;392:5–10. [PubMed: 9579855]

28. Konan YN, Berton M, Gurny R, Allemann E. Enhanced photodynamic activity of meso-tetra(4-hydroxyphenyl)porphyrin by incorporation into sub-200 nm nanoparticles. Eur J Pharm Sci 2003;18:241–49. [PubMed: 12659935]

29. McCarthy JR, Perez JM, Brückner C, Weissleder R. Polymeric nanoparticle preparation that eradicates tumors. Nano Lett 2005;5:2552–6. [PubMed: 16351214]

30. Ricci-Júnior E, Marchetti JM. Zinc(II) phthalocyanine loaded PLGA nanoparticles for photodynamic therapy use. Int J Pharm 2006;310:187–95. [PubMed: 16442755]

31. Esmaeili F, Hosseini-Nasr M, Rad-Malekshahi M, Samadi N, Atyabi F, Dinarvand R. Preparation and antibacterial activity evaluation of rifampicin-loaded poly lactide-coglycolide nanoparticles. Nanomedicine 2007;3:161–7. [PubMed: 17468055]

32. Jeong YI, Na HS, Seo DH, Kim DG, Lee HC, Jang MK, Na SK, Roh SH, Kim SI, Nah JW. Ciprofloxacin-encapsulated poly(dl-lactide-co-glycolide) nanoparticles and its antibacterial activity. Int J Pharm 2008;352:317–23. [PubMed: 18160236]

33. Shenoy D, Little S, Langer R, Amiji M. Poly(ethylene oxide)-modified poly(beta-amino ester) nanoparticles as a pH-sensitive system for tumor-targeted delivery of hydrophobic drugs. 1. *In vitro* evaluations. Mol Pharm 2005;2:357–66. [PubMed: 16196488]

34. Shenoy DB, Amiji MM. Poly(ethylene oxide)-modified poly(epsilon-caprolactone) nanoparticles for targeted delivery of tamoxifen in breast cancer. Int J Pharm 2005;293:261–70. [PubMed: 15778064]

35. Devalapally H, Shenoy D, Little S, Langer R, Amiji M. Poly(ethylene oxide)-modified poly(beta-amino ester) nanoparticles as a pH-sensitive system for tumor-targeted delivery of hydrophobic drugs: part 3. Therapeutic efficacy and safety studies inovarian cancer xenograft model. Cancer Chemother Pharmacol 2007;59:477–84. [PubMed: 16862429]

36. Panyam J, Zhou WZ, Prabha S, Sahoo SK, Labhasetwar V. Rapid endo-lysosomal escape of poly (DL-lactide-co-glycolide) nanoparticles: implications for drug and gene delivery. FASEB J 2002;16:1217–26. [PubMed: 12153989]

37. Tang W, Xu H, Kopelman R, Philbert MA. Photodynamic characterization and *in vitro* application of methylene blue-containing nanoparticle platforms. Photochem Photobiol 2005;81:242–9. [PubMed: 15595888]

38. Tada DB, Vono LL, Duarte EL, Itri R, Kiyohara PK, Baptista MS, Rossi LM. Methylene blue-containing silica-coated magnetic particles: A potential magnetic carrier for photodynamic therapy. Langmuir 2007;23:8194–9. [PubMed: 17590032]

39. Zeina B, Greenman J, Purcell WM, Das B. Killing of cutaneous microbial species by photodynamic therapy. Br J Dermatol 2001;144:274–278. [PubMed: 11251558]

40. Soukos NS, Mulholland SE, Socransky SS, Doukas AG. Photodestruction of human dental plaque bacteria: enhancement of the photodynamic effect by photomechanical waves in an oral biofilm model. Lasers Surg Med 2003;33:161–8. [PubMed: 12949945]

41. Bhatti M, MacRobert A, Meghji S, Henderson B, Wilson M. Effect of dosimetric and physiological factors on the lethal photosensitization of *Porphyromonas gingivalis in vitro*. Photochem Photobiol 1997;65:1026–31. [PubMed: 9188283]

42. Kömerik N, Wilson M. Factors influencing the susceptibility of gram-negative bacteria to toluidine blue-mediated lethal photosensitisation. J Appl Microbiol 2002;92:618–23. [PubMed: 11966901]
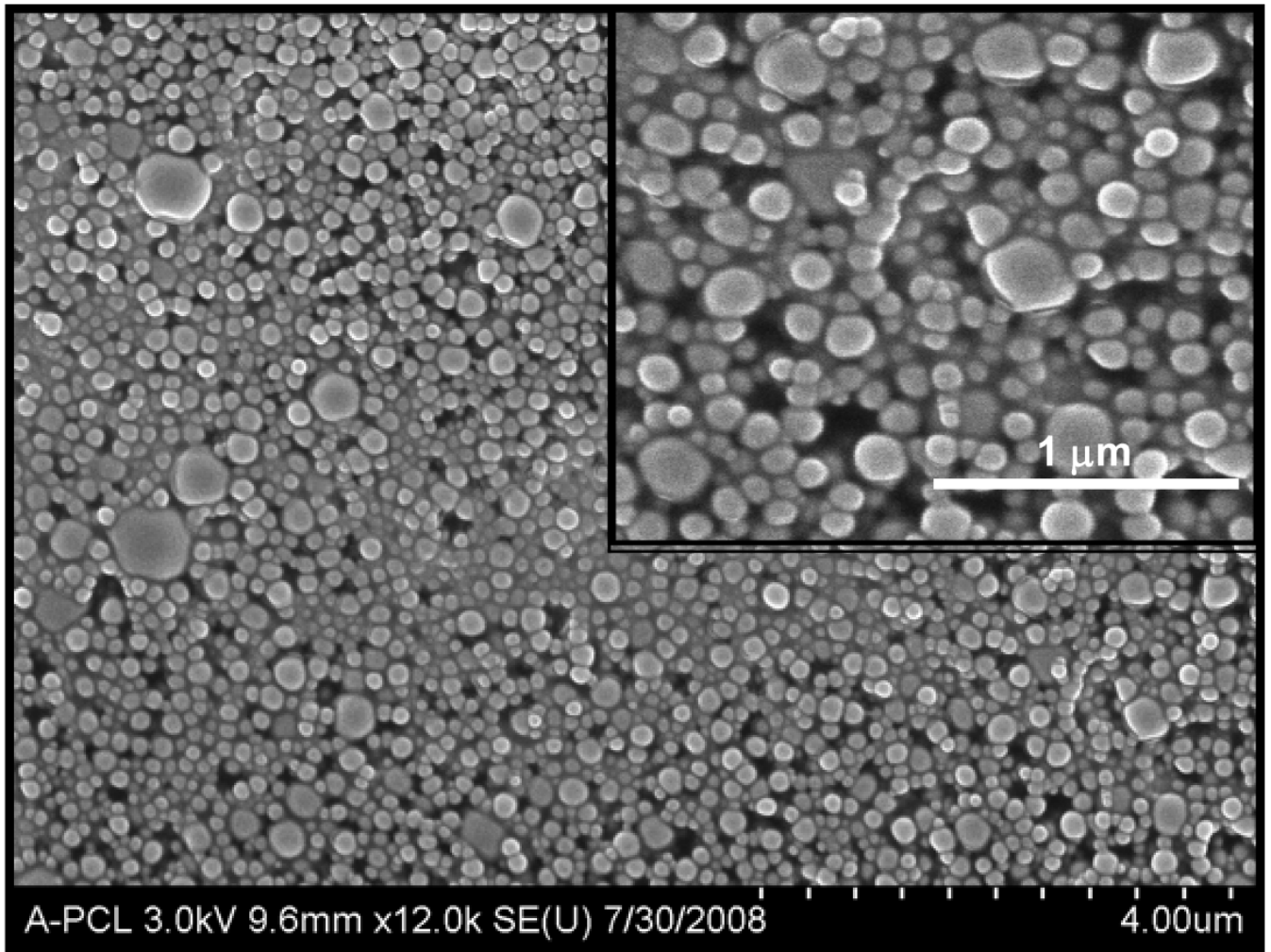
Figure 1.
Scanning electron micrograph (SEM) of blank PLGA nanoparticles. The inset shows an SEM image of higher magnification with spherical nanoparticles of 150–250 nm in diameter.
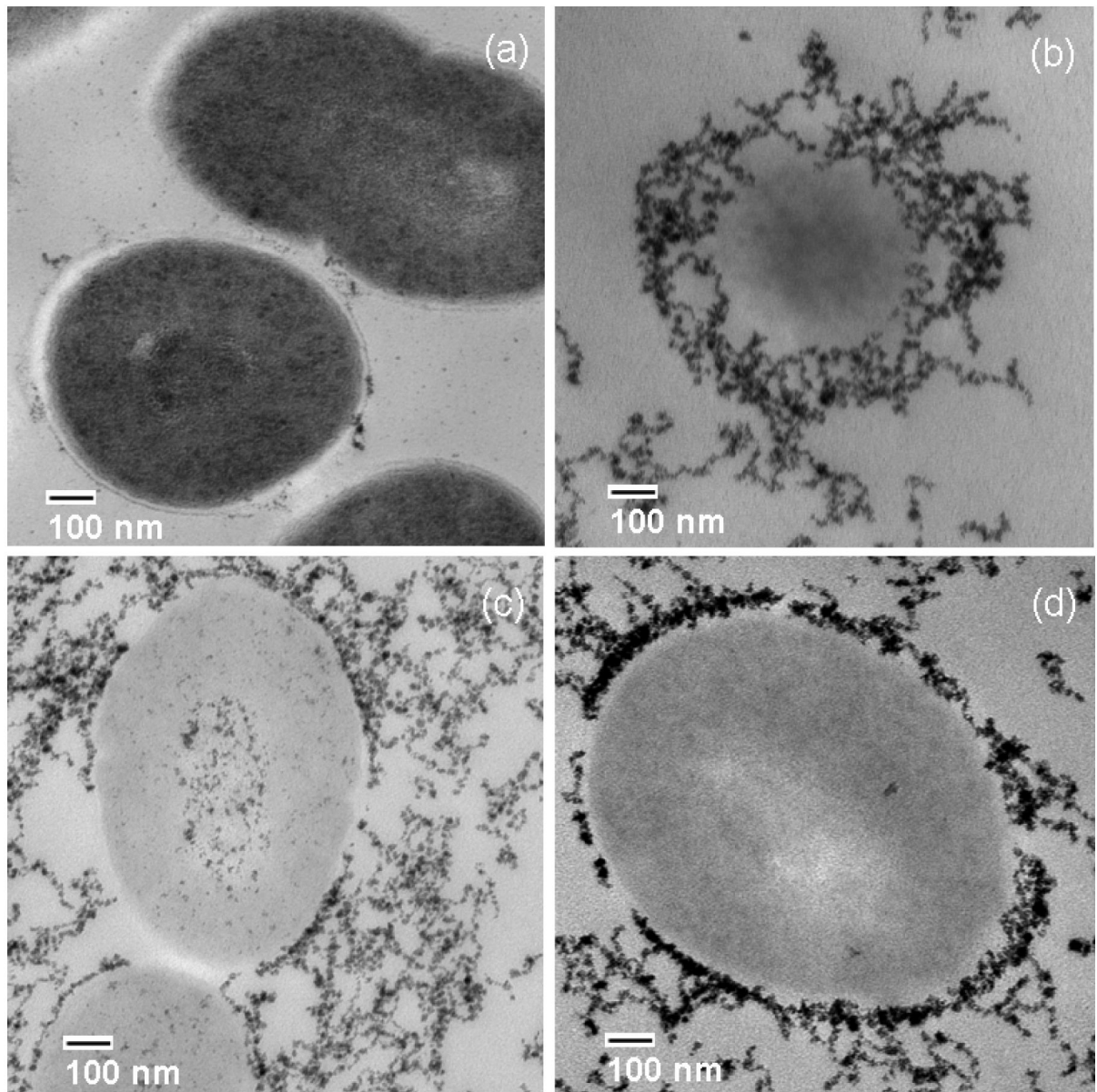
Figure 2.
Transmission electron microscopy of *E. faecalis* (a). Colloidal gold particles complexed with poly(lactic-*co*-glycolic acid) are concentrated mainly on the cell walls of microorganisms after 2.5 min (b), 5 min (c) and 10 min (d) of incubation.
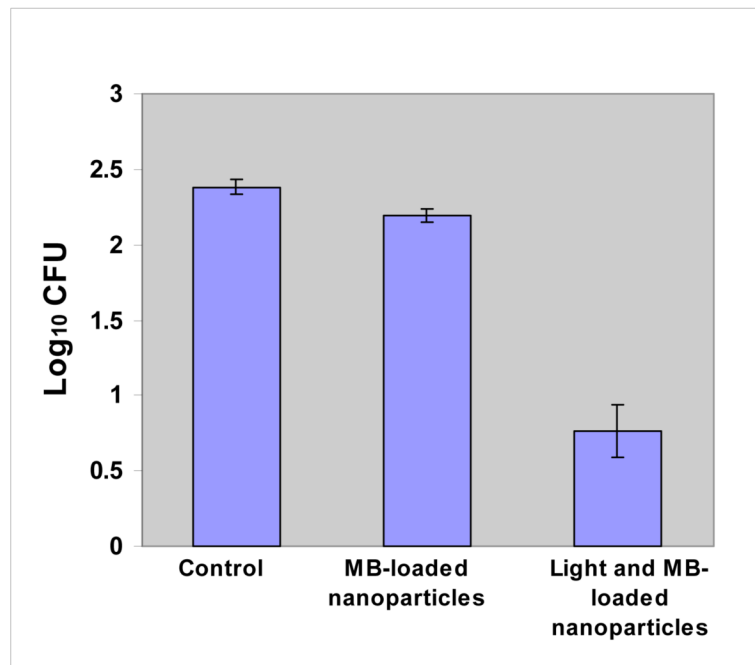
Figure 3.
Phototoxicity of *E. faecalis* species after incubation with MB-loaded PLGA nanoparticles (final concentration: 6.25 μg/ml equivalent to MB) for 10 minutes followed by treatment with red light of 665 nm (60 J/cm^2) and colony-forming assay. Each bar is the mean Log_{10} CFU levels (± Standard Error). The combination of light and MB-loaded nanoparticles was significantly lower than control or MB-loaded nanoparticles alone (pairwise comparisons of means by Tukey's procedure with overall alpha=0.01).
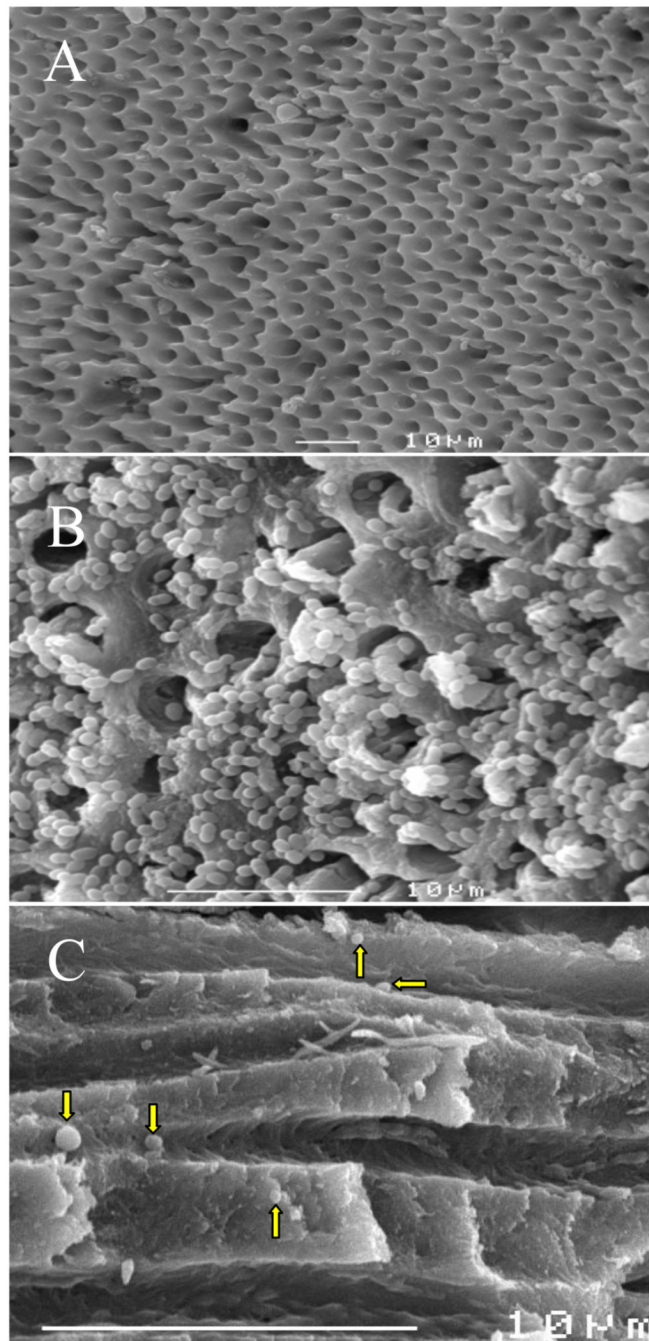
Figure 4.
Scanning electron microscopy. The root canal surface with the openings of dentinal tubules before infection with *E. faecalis* (A). *E. faecalis* biofilms on the pulpal canal wall and invasion of microorganisms into the dentinal tubules (B). Infiltration of dentinal tubules by MB-loaded nanoparticles (arrows, C).
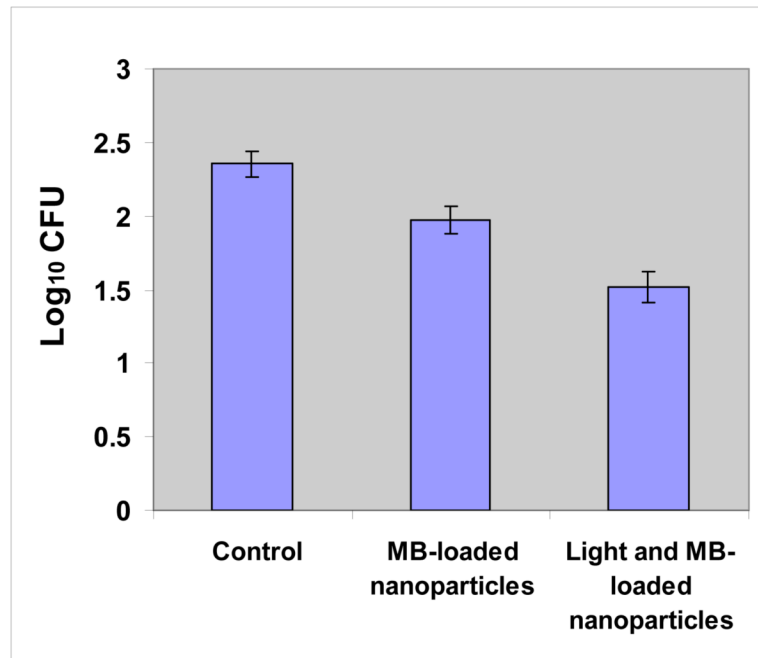
Figure 5.
Phototoxicity mediated in *E. faecalis*-derived root canal biofilms after incubation with MB-loaded PLGA nanoparticles (final concentration: 50 μg/ml equivalent to MB) for 15 min followed by exposure to red light of 665 nm (30 J/cm^2) and colony-forming assay. Each bar is the mean Log_{10} CFU levels (± Standard Error). The combination of light and MB-loaded nanoparticles was significantly lower than control or MB-loaded nanoparticles alone (pairwise comparisons of means by Tukey's procedure with overall alpha=0.01).